American Mineralogist, Volume 71, pages 396–405, 1986

Formation of tourmaline-rich gem pockets in miarolitic pegmatites

DAVID LONDON
School of Geology and Geophysics, University of Oklahoma, Norman, Oklahoma 73019

ABSTRACT

Analysis of fluid inclusions in spodumene, beryl, tourmaline, and quartz from miarolitic pegmatites of Afghanistan, coupled with lithium aluminosilicate stability relations and with previous studies from gem pegmatites of San Diego County, California, indicate that pocket development in tourmaline-rich, miarolitic rare-element pegmatites occurs between approximately 475 and 425°C and between 2800 and 2400 bars. This range of *P* and *T* is comparable to the conditions of late-stage crystallization in geochemically similar massive (nonmiarolitic) pegmatites. Whether gem pockets form may be dependent largely on the timing of tourmaline crystallization. Formation of tourmaline removes an alkali borate component from residual pegmatitic melt, with the consequent deposition of other alkali aluminosilicate and oxide-forming minerals and exsolution of copius amounts of H_2O. If tourmaline crystallization is inhibited until the late stages of pegmatite consolidation, the large quantities of H_2O that are liberated may form pegmatitic pockets.

INTRODUCTION

Much of the present understanding of pegmatite evolution is based on observations from subhorizontal, layered, gem-bearing miarolitic rare-element pegmatites (e.g., Jahns and Tuttle, 1963; Jahns and Burnham, 1969; Jahns, 1979, 1982). Pegmatites of this type are typically enriched in rare alkalis (Li, Rb, Cs); in Be, Sn, and Ta; and notably in tourmaline. They are chemically similar to more massive rare-element pegmatites such as the Tanco, Manitoba, and Harding, New Mexico, deposits. The best-studied miarolitic rare-element pegmatites are located in San Diego County, California (e.g., Jahns and Wright, 1951; Jahns and Tuttle, 1963; Foord, 1976, 1977; Jahns, 1979; Taylor et al., 1979), but these deposits are typical of miarolitic pegmatites elsewhere that are less well known (e.g., in the Hindu Kush of Afghanistan and Pakistan: Rossovskii, 1977, 1981; Rossovskii and Shmakin, 1978; Rossovskii et al., 1975, 1978). In this paper, the *P-T* conditions and fluid evolution of rare-element miarolitic pegmatites are evaluated in the light of recent fluid-inclusion studies and phase-equilibrium experiments, because deposits of this type have had such a profound effect on models for internal evolution of pegmatite systems (Jahns and Burnham, 1969; Burnham and Nekvasil, 1986). This investigation of miarolitic pegmatites draws heavily on two previous studies: experimental calibration of the lithium aluminosilicate phase diagram (London, 1984a), and a study of fluid inclusions in the Tanco pegmatite, Manitoba (London, 1986). These works provide the framework by which previous investigations of miarolitic pegmatites can be reevaluated, and they serve as the basis for analysis of new data from miarolitic pegmatites in the Hindu Kush of Afghanistan.

GEOLOGY

The geology of miarolitic rare-element pegmatites of this type is sufficiently similar worldwide that the typical mineralogical and zonal characteristics can be summarized in the diagram that serves as the logo for this issue (Jahns and Burnham, 1969; Ford, 1976, 1977) (Fig. 1). The pegmatites generally display a layered rather than concentric zonation, with predominantly banded albitic aplites on the footwalls, coarse microcline-quartz pegmatite on the hanging walls, and interior units that consist principally of coarse-grained cleavelandite, tourmaline, microcline, quartz, and fine-grained micas. More exotic accessories such as beryl, spodumene, Nb-Ta-Sn-(±Bi) oxides, and phosphates are concentrated in the quartz- or cleavelandite-rich interior zones. Trace-element distributions (especially of Li, Rb, and Cs) are generally consistent with a model of inward sequential crystallization, although Jahns (1982) recognized that some mineralogically distinct internal units may crystallize simultaneously (cf. Walker, 1985; Jolliff et al., 1986).

Most miarolitic gem-bearing pegmatites contain spodumene in assemblage with quartz in massive, primary units and as pocket constituents (e.g., the Afghanistan Hindu Kush: Rossovskii, 1981; Rossovskii et al., 1975; San Diego County, California: Jahns, 1949; the Rumford-Newry area, Maine: Cameron et al., 1954; and Minas Gerais, Brazil: Cassedanne and Cassedanne, 1981). This observation constrains the *P-T* conditions of primary crystallization and pocket formation in miarolitic pegmatites to lie within the stability field of the assemblage spodumene + quartz (London, 1984a). The spodumene within these pegmatites is nearly pure $LiAlSi_2O_6$ (e.g., see analysis in Table 1 of London, 1984a, and analyses of spodumene

0003–004X/86/0304–0396$02.00

from other massive and miarolitic pegmatites in Table 5 of London and Burt, 1982), so that the stability field for spodumene is not displaced to higher temperatures and lower pressures by extensive solid solution (cf. Appleman and Stewart, 1968; London, 1984a). The experimental work on which the lithium aluminosilicate phase diagram (London, 1984a) is based utilized natural pocket spodumene from the Hindu Kush pegmatites (London, 1984a, Table 1); thus, this diagram is directly applicable to natural mineral equilibria. Note also that the applicability of the lithium aluminosilicate phase diagram depends only on the presence of a lithium aluminosilicate phase, not on its abundance.

KULAM PEGMATITES, AFGHANISTAN

Miarolitic gem pegmatites that contain abundant spodumene, beryl, and tourmaline lie in the Hindu Kush of eastern Afghanistan (Fig. 2), and they are geologically similar to miarolitic pegmatites elsewhere (Rossovskii, 1981; Rossovskii et al., 1975, 1978). The Afghanistan miarolitic pegmatites occur mostly in the roof zones of biotite-muscovite granites. The peak metamorphic grade attained by surrounding metasedimentary rocks was medium-pressure amphibolite grade, as shown by garnet-staurolite-cordierite-andalusite assemblages in metapelites (Rossovskii et al., 1978).

Rossovskii et al. (1978) reported the following paragenesis of pocket minerals. Two generations of spodumene were noted: (1) coarse-grained (primary) spodumene embedded in massive quartz, microcline, and cleavelandite and (2) kunzite (gem spodumene) in miarolitic pockets. Primary spodumene and microcline served as the substrate for deposition of kunzite. Quartz, beryl, tourmaline, and other accessory phases encrust kunzite crystals and were the latest-formed phases. Samples of spodumene, beryl, tourmaline, and quartz from the Kulam deposit were obtained from collections of the Smithsonian Institution, the American Museum of Natural History, and from private mineral dealers for examination of fluid inclusion properties and for comparison with the reported results of fluid-inclusion studies from the San Diego pegmatites. Rossovskii (1977, 1981; Rossovskii et al., 1978) presented a partial analysis of fluid inclusions from this pegmatite field.

Properties of fluid inclusions

Fluid inclusions are present in all phases studied and possess several uniform similarities and differences. In all samples, the abundance of fluid inclusions decreases from crystal base to tip. Solid inclusions with no associated fluids are abundant at the bases and outer margins of crystals.

Equation (2) of Potter et al. (1978) was used to calculate salinities of aqueous fluids. Densities of homogeneous aqueous fluids were calculated from equation (Al) of Bodnar (1983). Isochores were constructed by comparison to pertinent graphical data in Fisher (1976) and in Roedder and Bodnar (1980).

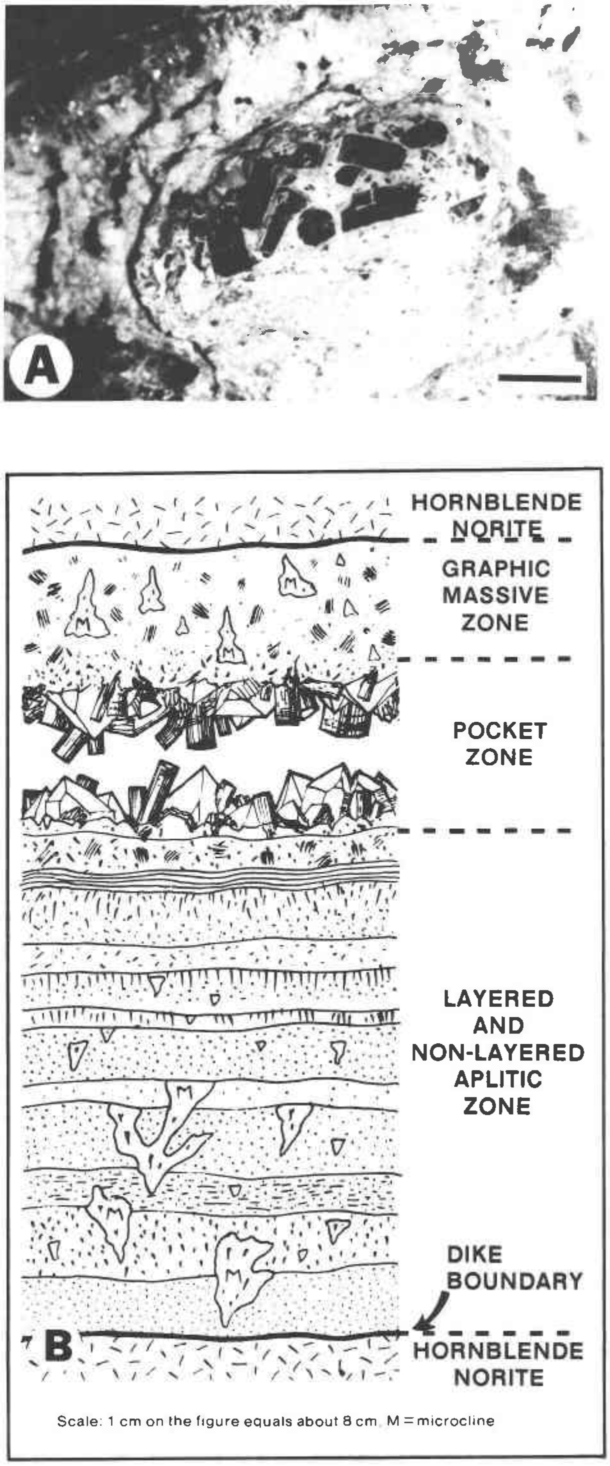

Fig. 1. (A) Tourmaline-rich pocket from the Himalaya dike, San Diego County, California. Dark prisms within the pocket are crystals of elbaite. The scale bar is 10 cm. (B) Schematic cross section through the Himalaya dike, San Diego County, California. Both figures reprinted from Foord (1977) by permission of the author.

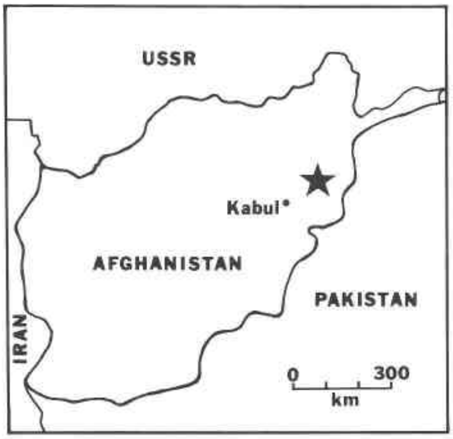

Fig. 2. Location of the miarolitic pegmatites (star) of Afghanistan. The pegmatites are located near Nuristan in the Laghman province; individual pegmatite groups are referred to by the location names Kulam, Mawi, Nilaw, and Kurgal.

Microthermometry was performed on a Linkam TH 600 programmable heating and freezing stage at the University of Oklahoma. The Linkam stage was calibrated with respect to melting points of 25 standard or spectroscopic-grade compounds over the range −57°C to +307°C. Dissolution of aluminosilicate minerals within inclusions was accomplished by sealing polished chips in Pt foil for runs at $P = 2$ kbar (to prevent decrepitation of inclusions). The progress of dissolution was monitored by examination of the proportions of crystals to glass upon quench. For daughter-mineral assemblages, minimum entrapment temperatures are defined by the run temperatures from which quenched products include only glass plus aqueous fluids.

Most fluid inclusions contain low-salinity aqueous fluids and no other detectable volatile components (e.g., CO_2). On the basis of freezing-point depression (T_m ice), the salinites of the aqueous component in most inclusions range from 0.9 to 7.9 wt% (mean = 3.7) NaCl equivalent (Fig. 3A). The low salinities preclude an accurate measurement of eutectics (first appearance of liquid upon heating a frozen inclusion). Samples of spodumene, beryl, and quartz contain two or more generations of fluid inclusions (Fig. 4). Most inclusions in spodumene and beryl are crystal-rich, whereas inclusions in quartz and tourmaline contain no solid phases.

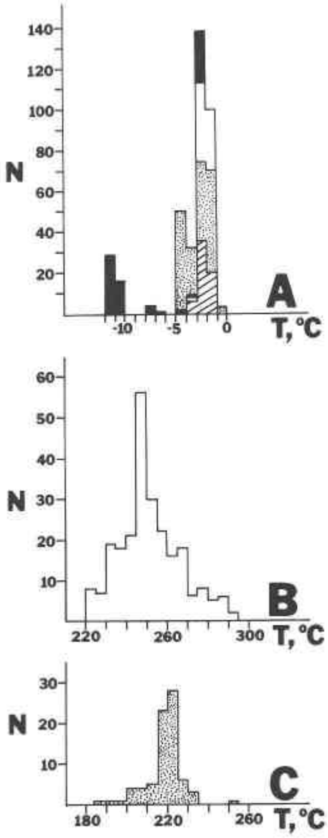

Fig. 3. Histograms of microthermometric data for inclusions in spodumene (white bars), beryl (stippled bars), quartz (black-bars), and tourmaline (ruled bars) from the Kulam pegmatites, Afghanistan. (A) Freezing-point depression of aqueous liquid (T_m ice; bar graphs superimposed, not stacked); (B) temperatures of liquid-vapor homogenization (T_h LV) for crystal-rich inclusions in spodumene, and (C) temperatures of liquid-vapor homogenization (T_h LV) for crystal-rich inclusions in beryl.

Spodumene and beryl. In spodumene and beryl, large inclusions with slightly irregular negative crystal forms of the host phases are particularly crystal-rich (Fig. 4). Electron energy-dispersive (EDS) analyses of opened inclusions reveal a fairly consistent assemblage of quartz, albite, cookeite, and pollucite, cassiterite, and microlite or rynersonite (Ca-Ta oxide). In addition, most inclusions contain other nonsilicate minerals that are not yet fully identified. One such prismatic phase shows only phosphorus by EDS and, hence, appears to be a lithium or beryllium phosphate or crystalline phosphoric acid (Fig. 4). An unidentified hairlike acicular phase is present in virtually all inclusions (Figs. 4D, 4J). Some of the nonsilicate phases dissolve prior to decrepitation at 275–350°C. The aluminosilicate minerals show no evidence of dissolution up to decrepitation. Dissolution of aluminosilicate minerals (as monitored by quenched runs from 2 kbar; see London, 1986, for methodology) begins at approximately 375°C and is essentially complete in most inclusions by 500°C. These crystal-rich inclusions are cut and modified by later generations of inclusions with few to no crystalline solids but similar aqueous-fluid salinities (Fig. 3).

As a whole, temperatures of liquid-vapor homogenization show considerable scatter, but consistent trends emerge when inclusion populations are sorted on the basis of crosscutting relationships. The crystal-rich inclusions in spodumene and beryl generally possess the highest average values and narrowest spread of T_h LV (temperature of liquid-vapor homogenization; Figs. 3A, 3B). In a few spodumene crystals, T_h LV and the crystal/fluid ratio of inclusions decrease from crystal base to tip. In spodumene and beryl, the younger crystal-poor or crystal-absent in-

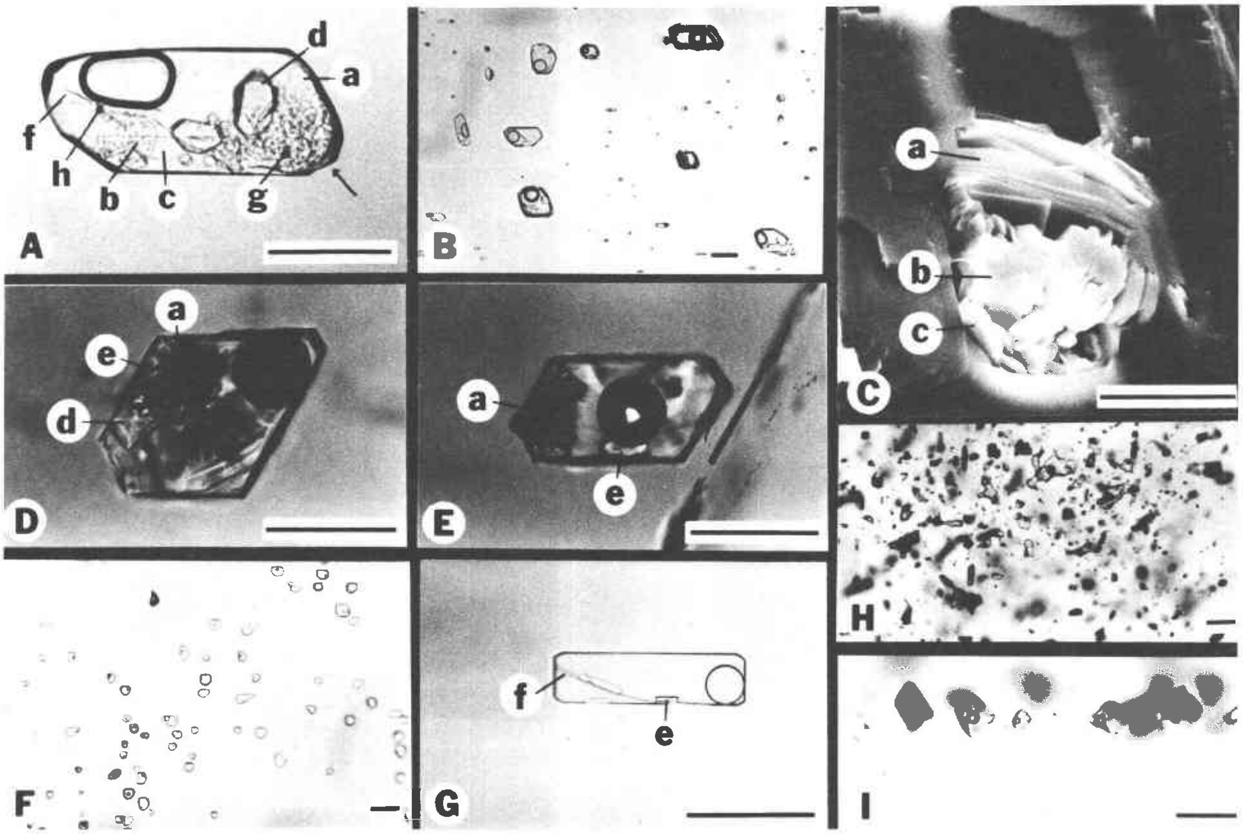

Fig. 4. Fluid inclusions in spodumene (A–C), beryl (D–G), and quartz (H–I) from the Kulam pegmatite, Afghanistan. In spodumene, inclusions at the bases of some crystals contain a higher proportion of daughter minerals (A) than inclusions at the crystal tip (B); in A, the inclusion shape has changed slightly from a rounded surface against which daughter minerals were precipitated to a more regular negative-crystal form (arrow). Daughter minerals in the SEM image (C) and in the unopened inclusions are (a) cookeite, (b) pollucite, (c) albite, (d) quartz, (e) a birefringent light-element (Li, Be, or H) phosphate, (f) an unidentified hairlike phase, and (g, h) cassiterite and microlite or rynersonite. Most crystal-rich inclusions in spodumene contain both Sn- and Ta-oxides, but the identity of the individual grains cannot be ascertained within unopened inclusions. The daughter-mineral assemblage in inclusions near the tips of spodumene crystals (B) is comparable to that of crystal-rich inclusions in beryl (D–E). In E, the (001) plane that contains the large, crystal-rich inclusion is cut by a fracture that contains crystal-poor or crystal-absent inclusions such as those in F and G; note the variability of liquid/vapor ratios (at 25°C) of inclusions in F. Most inclusions in quartz have irregular forms and variable liquid/vapor ratios at 25°C (H); rarely, healed fractures contain two-phase aqueous inclusions with regular negative-crystal forms, comparatively high salinity, and uniform liquid/vapor ratios (I). Dense clusters of low-salinity inclusions (H) are abundant toward the bases of quartz crystals, whereas the high-salinity inclusions along obvious fractures (I) occur only toward the tips. Scale bar in all photos is approximately 30 μm.

clusions display extremely variable T_h LV (ranging from inclusions that contain no vapor bubble at 25°C to those in the same cluster that decrepitate at temperatures up to 400°C prior to T_h LV) (Fig. 4I).

Tourmaline and quartz. In contrast to spodumene and beryl, inclusions in tourmaline and quartz generally contain no crystalline phases and have irregular shapes and variable size (e.g., Fig. 4K). Fluid compositions and apparent salinities are similar to those in spodumene and beryl; however, like the later-stage inclusions in spodumene and especially beryl, the liquid-vapor ratios of inclusions in tourmaline and quartz are highly variable (Fig. 4K) and preclude any meaningful determination of T_h LV. Some samples of quartz contain healed fractures with large, euhedral inclusions that possess unusually high salinity (15 wt% NaCl equivalent) and a low but narrow range of T_h LV = 217 ± 1 (s.d.)°C (n = 42) (Figs. 3, 4L).

Interpretation of inclusion data

The overall uniformity of the crystalline assemblage within inclusions hosted by spodumene and beryl suggests that most of these phases are daughter minerals rather than accidentally entrapped solids. Phase assemblages and crystal-fluid ratios do vary slightly between inclusions within a given cluster (e.g., Figs. 2A, D). Necking down of large inclusions during or after deposition of crystalline solids may explain the variations. Evidence of postentrapment modification is manifest by inclusions such as the one shown in Fig. 4B; the rounded edge of included solids illustrates that the original shape of the inclusion

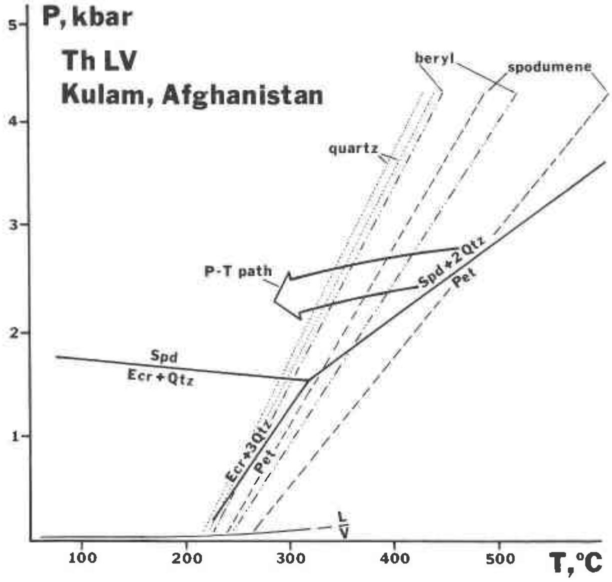

Fig. 5. Estimated conditions of pocket formation in miarolitic pegmatites of Kulam, Afghanistan (arrow), based on isochores (T_h LV, partial homogenization) for spodumene and beryl constructed from microthermometric data in Fig. 3. The isochore for inclusions in quartz is derived from the microthermometric properties of the inclusions shown in Figure 4I. Phase abbreviations are eucryptite (Ecr), spodumene (Spd), petalite (Pet), quartz (Qtz), low-salinity (5 wt% NaCl) aqueous liquid (L) plus vapor (V).

has changed to a more regular negative-crystal form. The variations in daughter-mineral assemblages, however, are greater between samples than within a single crystal. One possible explanation for these differences is that individual crystals may have come from different pockets. Isolation of residual pegmatitic magma in a compositionally heterogeneous and largely crystallized pegmatite could lead to significant differences in pocket zone composition and mineralogy. Rossovskii et al. (1978) reported that the mineralogy is highly variable from pocket to pocket. Alternatively, the variability of pocket-mineral assemblages could be interpreted to reflect the segregated growth of different mineral phases in portions of interconnected residual pegmatitic fluid.

The crystal-rich inclusions are distinctly different from accidentally trapped solids. For example, fringes of tourmaline needles that surround the margins of some beryl crystals are randomly oriented on the former beryl surfaces and contain no associated fluids.

The crystal-rich aqueous inclusions in spodumene and beryl are regarded as modified but possibly primary inclusions that reflect entrapment of an alkali aluminosilicate-rich fluid. These inclusions are the earliest set that was entrapped, because they are crosscut by planes of crystal-poor or simple liquid-vapor inclusions. Isochores for crystal-rich inclusions in beryl (T_h LV, partial homogenization) reflect lower temperatures of entrapment than similar inclusions in spodumene (Figs. 4 and 5), which is consistent with the observation of Rossovskii et al. (1978) that beryl encrusts kunzite crystals and hence formed later than the spodumene. The crystallization of spodumene early in pocket development (Rossovskii et al., 1978) may explain why inclusions in this phase contain a higher proportion of daughter minerals. There is no textural evidence that any of the simple liquid-vapor inclusions in any phase are primary. As pointed out by Roedder (1981), however, the fact that pocket minerals are euhedral, smooth-faced, and project into voids implies that the final medium from which such crystals grew must have been a fairly aluminosilicate-poor fluid. Although the simple aqueous inclusions are extensively modified, the fluids contained by them probably are indigenous to the pegmatite. Their compositions are distinctly different from the saline, CO_2-rich inclusions that are typical of most metamorphic rocks (e.g., Hollister and Burruss, 1976; Touret, 1981).

The changes in daughter-mineral assemblages in sequential populations of inclusions in spodumene and beryl may be used to evaluate the crystallization sequence in the Kulam pegmatite pockets. From the sequence of crystal-rich to crystal-poor inclusions in spodumene, the phases quartz, albite, microlite/rynersonite, and cassiterite appear to have crystallized first, followed by pollucite and finally cookeite with several other nonsilicate minerals (of which one is a light-element phosphate). Crystal-rich inclusions in beryl generally contain little or no quartz, albite, and oxides. This appears to confirm the observation of Rossovskii et al. (1978) that beryl crystallized after spodumene but with some temporal overlap. Rossovskii et al. (1978) did not identify light-element phosphates and other comparatively soluble nonsilicates from the Kulam pocket assemblages. Roedder (1981), however, has noted that soluble phases that may have once occupied miarolitic pockets may have been dissolved by circulation of connate or meteoric water after pocket formation. The detailed mineralogical investigation by Foord et al. (1986) identified borates and carbonates within pockets of the San Diego pegmatites.

A phase that optically and morphologically resembles $Li_2B_4O_7$ (see London, 1986) is present in some crystal-rich inclusions in the Kulam pocket minerals, but such a light-element phase has not been observed in the SEM and EDS analysis of opened inclusions. It is doubtful that $Li_2B_4O_7$ would be present in the crystal-rich inclusions in the Kulam spodumene from the pocket zones, because the fluids in these pockets are equilibrated with tourmaline, whereas those in the spodumene from Tanco were not (London, 1986).

Isochores constructed from microthermometric properties (partial homogenization) of the crystal-rich inclusions in spodumene project into the stability field of spodumene + quartz (Fig. 5). These inclusions, which appear to be the earliest trapped, may reflect the conditions at the onset of pocket formation. From the experimental homogenization of aluminosilicate daughter minerals within spodumene-hosted inclusions, pocket formation may have begun at temperatures of approximately 475–

500°C. At 475°C, the pressures within pockets would have been approximately 2600 bars (within the stability field of spodumene + quartz; Fig. 5). From 475°C and 2600 bars, the successive populations of inclusions in spodumene and beryl define an interval from approximately 475 to 340°C over which pockets were generated. On the basis of inclusions in quartz, tourmaline, and beryl, the aluminosilicate components of the primary pocket-forming fluids were depleted by 350–400°C. The succession of inclusions from spodumene to beryl to quartz and the crosscutting relations of secondary inclusions in spodumene and beryl record a continuous change from silicate-rich to silicate-poor aqueous fluid during pocket formation. The limited microthermometric data for secondary, solute-poor liquid-vapor inclusions in quartz (Fig. 3) are suggestive of extensive fracturing and rehealing of pocket minerals at clearly subsolidus conditions.

The proposed *P-T* interval for formation of pocket minerals in the Kulam, Afghanistan, pegmatites may be compared to the conditions of late-stage crystallization in the Li-rich Tanco pegmatite, Manitoba (London, 1986). At Tanco, a hydrous borosilicate fluid evolved through crystallization to a comparatively low-density, solute-poor aqueous liquid over the ranges of 470 to 420°C and 2700 to 2600 bars. The crystalline products of this fluid included spodumene, quartz, albite, Li-micas, tourmaline, beryl, pollucite, and Ta-Sn oxides. This is essentially the same mineralogical assemblage that is reported from miarolitic pockets in the Kulam pegmatites and elsewhere (e.g., Jahns and Wright, 1951; Cameron et al., 1954; Foord, 1976, 1977; Jahns, 1979, 1982; Cassedanne and Cassedanne, 1981). It appears that (1) the bulk compositions and liquid lines of descent of late-stage fluids in the massive Tanco pegmatite and the miarolitic Kulam pegmatites were similar; (2) the *P-T* conditions over which these fluids crystallized and evolved an aqueous-fluid phase were virtually identical; and (3) the changes in crystal-fluid phases over this interval mark the transition from magmatic to hydrothermal conditions in massive and miarolitic pegmatites with similar Li- and B-rich bulk compositions.

Some of the most important observations from this study pertain to the properties and interpretation of fluid inclusions in pegmatite minerals. The examination of fluid inclusions in pocket minerals from the Kulam pegmatites facilitates an important comparison with observations from the Tanco pegmatite (London, 1986). In both deposits, inclusions in spodumene are crystal rich and possibly primary, whereas those in quartz are crystal poor and are secondary. This disparity in the compositions of inclusions in spodumene versus quartz appears to be characteristic of other rare-element pegmatites, such as the Bikita deposit, Zimbabwe (D. London, unpub. data, 1985). These observations reinforce the contention that pegmatitic quartz generally does not trap primary fluid inclusions, and that the examination of inclusions hosted by quartz only may lead to an erroneous interpretation of fluid compositions and *P-T* conditions of pegmatite formation (London, 1985). The reason for this difference in behavior is not known. Spodumene (and phases such as beryl and topaz) may be more refractory or insoluble than quartz, and hence preserve inclusions trapped at higher *P* and *T*. There is no evidence from any of the pegmatites studied that quartz ever entrapped the silicate-rich fluids that are represented by inclusions in spodumene and beryl from the Kulam pegmatites (i.e., solid inclusions that may once have been daughter minerals are not found in quartz).

The prevalence of liquid-vapor inclusions in tourmaline may reflect a secondary origin, as in quartz, or may be related to the local generation of an aqueous fluid during the formation of tourmaline. Individual tourmaline crystals may act as centers for production of an aqueous-fluid phase because of the large quantities of H_2O liberated by tourmaline-forming reactions. Development of an aqueous boundary fluid would most likely occur along the surfaces perpendicular to [0001], the zone of fastest growth in tourmaline. As in the San Diego pegmatites (Foord, 1976), modified fluid inclusions in the Afghanistan tourmaline lie mostly in planes perpendicular to [0001].

SAN DIEGO COUNTY PEGMATITES, CALIFORNIA

Taylor et al. (1979) combined studies of fluid inclusions and oxygen-, hydrogen-, and carbon-isotope systematics to deduce the conditions of formation for three of the best-known gem-bearing pegmatites of the San Diego County field, the Himalaya, the Tourmaline Queen, and the Stewart dikes (Foord, 1976; Taylor et al., 1979). From the isotope systematics, they concluded that the pegmatitic magmas were emplaced at temperatures of 700–730°C, with pocket formation at subsolidus conditions in the range of 525–565°C. An estimate of emplacement pressure was calculated by determination of the pressure required to correct a liquid-vapor homogenization temperature in aqueous fluid inclusions to the temperature of pocket formation as defined by the isotope systematics (see Roedder and Bodnar, 1980, for details of methodology). For this purpose, Taylor et al. (1979) chose to base the pressure correction on the microthermometric properties of a fluid inclusion with the highest liquid-vapor homogenization temperature (340°C from an inclusion in a spessartine-almandine garnet). On this basis, the pressure at crystallization was estimated at 2100–2200 bars. The bulk of inclusions in pocket quartz, tourmaline, beryl, apatite, and stibiotantalite, however, possessed lower average liquid-vapor homogenization temperatures (T_h LV) of 285–295°C. The abundant crystalline contents of the inclusions (which were regarded as daughter minerals) were not homogenized, and their contribution to fluid chemistry was not considered.

In Figure 6, it is apparent that the previously estimated *P-T* conditions for the San Diego pegmatites lie well in the petalite + quartz field, approximately 150°C or 1500 bars beyond the limits of the spodumene + quartz field. Several of the San Diego pegmatites, including the Himalaya, Stewart, and six other dikes, contain spodumene + quartz, but no petalite (Jahns, 1979). Either the isotopic

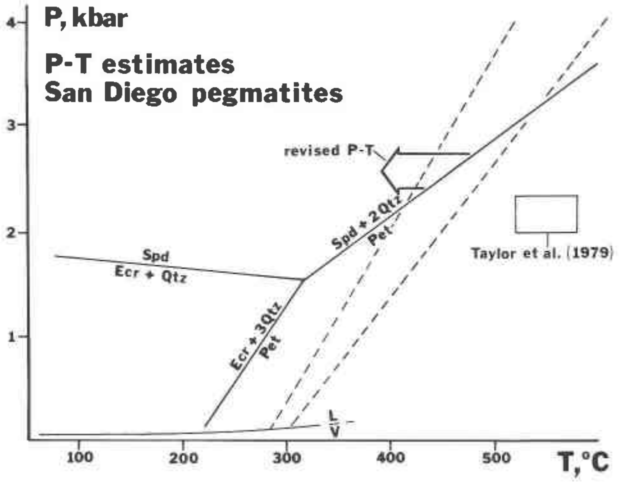

Fig. 6. Pressure-temperature estimates for the San Diego County pegmatites, California. The estimated *P-T* conditions of Taylor et al., (1979) are represented by the box. A revised estimate (arrow) is based on isochores (dashed lines) constructed from microthermometric data in Foord (1976) and Taylor et al. (1979) and is consistent with lithium aluminosilicate assemblages in these pegmatites—as constrained by the lithium aluminosilicate phase diagram of London (1984a; solid reaction lines)—and with *P-T* estimates of peak regional metamorphism. Phase abbreviations are eucryptite (Ecr), spodumene (Spd), petalite (Pet), quartz (Qtz), low-salinity (5 wt% NaCl) aqueous liquid (L) plus vapor (V).

temperature or the interpretation of the fluid-inclusion data (or both) appears to be in error. From the reported salinity of 4–5 wt% NaCl equivalent (Foord, 1976; Taylor et al., 1979) and the average T_h LV = 290°C for most pocket minerals, isochores for the aqueous component of fluid inclusions from the San Diego pegmatites intersect the isotopic equilibration temperature of 525–560°C at minimum pressures of 2800–3300 bars. This *P-T* condition lies outside of or marginally within the spodumene + quartz field. At some of the San Diego pegmatites (e.g., the Stewart dike), as in the miarolitic pegmatites of Afghanistan, Brazil, and the Rumford-Newry district of Maine, primary spodumene crystallized prior to pocket development; thus, these pegmatites should have been well into the stability field of spodumene + quartz at the time of pocket formation. In addition, the resultant pressure estimates for the San Diego pegmatites are higher than those for the Afghanistan pegmatites and are at the upper boundary for the inferred peak metamorphic pressures for the western portion of the Peninsular Ranges batholith and included metamorphic rocks (which reflect greenschist-amphibolite facies conditions, but with andalusite-cordierite assemblages in some metapelites; e.g., Todd and Shaw, 1979).

The oxygen-isotope fractionation between quartz-feldspar, quartz-muscovite, quartz-garnet, and garnet-muscovite show considerable scatter that is especially great for pocket-zone minerals. Taylor et al. (1979) attributed these variations to isotopic re-equilibration that was more extensive in pocket zones. In their calculation of isotopic equilibrium temperatures, Taylor et al. (1979) omitted a number of points from the linear regression of the data, partly on the basis that these values gave temperatures of equilibration that were regarded as "unreasonably" low for pocket formation (e.g., Taylor et al., 1979, Fig. 6B). If the temperatures of formation of tourmaline-rich pockets are revised downward to 425–475°C, then correspondingly, pressures in the range of 2400–2800 bars would satisfy the constraints of the lithium aluminosilicate assemblage, the bulk of Foord's (1976) fluid-inclusion data, and the approximate pressures of regional metamorphism. The lower temperatures for primary pocket formation also provide continuity with the conditions of ensuing hydrothermal alteration, estimated by Foord et al. (1986) to have spanned the interval of 150–400°C.

DISCUSSION

P-T conditions of pocket formation

The available fluid inclusion data from the Kulam and San Diego pegmatites, coupled with the ubiquitous assemblage spodumene + quartz, constrain the conditions of pocket formation to the approximate ranges of 425–475°C and 2400–2800 bars, which is consistent with all types and sources of data except the isotopic temperature reported by Taylor et al. (1979). This *P-T* range for late-stage primary crystallization is comparable to that of the Tanco pegmatite, Manitoba (London, 1983, 1986) and signifies that compositionally similar miarolitic and massive rare-element pegmatites may crystallize under similar *P-T* conditions. The development of miarolitic pockets in pegmatites is contingent on factors other than *P-T* conditions of emplacement.

Causes of pocket formation

Miarolitic pockets provide incontrovertible evidence for the exsolution of a comparatively low-density aqueous fluid from silicate melt during the late stages of pegmatite genesis. Crystal-lined cavities such as those cited by Jahns (1979, 1982) are primary (although subsolidus alteration is common). In view of the conclusion that miarolitic and massive pegmatites crystallize at similar *P-T* conditions, the presence or absence of pegmatitic pockets appears to be controlled by the timing and extent of volatile exsolution from silicate melt.

Fluid-inclusion data from this and previous studies (e.g., Taylor et al., 1979; London, 1986) reveal that the salinities (i.e., chloride content) of typical rare-element pegmatites are low. Exsolved late-stage aqueous fluids generally contain less than 4 wt% NaCl equivalent. Low-salinity aqueous fluids are incapable of transporting large quantities of dissolved aluminosilicate components (e.g., Anderson and Burnham, 1967; Burnham, 1967). In particular, the solubility of Al is markedly suppressed in chloride-bearing solutions (Anderson and Burnham, 1967; Burnham and Nekvasil, 1986), yet pocket-zone minerals (e.g., beryl, tourmaline, spodumene) are distinctly Al-rich. The precipitation of primary pocket silicates from a low-salinity aqueous fluid requires either a large water/rock ratio or extensive fluid recirculation during pocket formation. Evidence cited by London (1985) argues against either of these conditions during pegmatite consolidation (see also Jahns, 1982; Norton, 1983; Walker, 1985). It appears that pocket-zone aluminosilicate minerals crystallize from hydrous silicate-rich fluids that may be in contact with an exsolving aqueous phase, but that the solute-poor aqueous fluid (represented by inclusions in pocket quartz) does not constitute the bulk composition of the medium from which pocket minerals crystallize.

The abundance of tourmaline in pegmatitic miaroles (Fig. 1) reflects high concentrations of boron in late-stage pegmatitic fluids and provides an important clue for understanding pocket formation. Although variable in abundance, tourmaline may form more than 50 vol% of pockets (e.g., see Fig. 1A); thus, pockets contain a large proportion of the boron that was originally present in the pegmatitic magmas, and that boron was retained in fluids until the late stages of pegmatite consolidation.

Addition of boron to aluminosilicate melts (1) significantly enhances the miscibility of silicate melt and H_2O (e.g., Chorlton and Martin, 1978; Pichavant, 1981, 1983; London, 1984b, 1986), (2) lowers melt viscosity and increases the solubility of incompatible trace elements (Bonniaud et al., 1978; London, 1986), and (3) promotes rapid crystal growth (London, 1986). Fluid inclusions in spodumene from the Tanco pegmatite provide direct evidence for high concentrations of boron and rare elements in late-stage hydrous silicate fluids (London, 1984b, 1986). In the San Diego County pegmatites, Foord et al. (1986) recognized additional evidence for high boron concentrations in residual liquids: (1) tourmalinization of wall rock adjacent to pockets (in some cases, a direct relation to aplitic dikes that emanate from pockets) and (2) anomalously high boron contents (2–3 wt% boron) of aplitic feldspars in pocket zones.

The role of boron and tourmaline as elucidated by London (1986) in the massive Tanco pegmatite appears to be applicable to miarolitic pegmatites as well. The crystallization of tourmaline consumes the fluxing alkali borate component (lithium or sodium tetraborate) of late-stage pegmatitic melts, which leads to a consequent rise in the solidus temperature of the residual aluminosilicate fluid, resultant precipitation of aluminosilicate and oxide-forming minerals (e.g., Nb–Ta–Sn oxides), and exsolution of H_2O. For example, $Li_2B_4O_7$-bearing fluid inclusions from the Tanco pegmatite contain approximately 2 mol of H_2O per mole of aluminosilicate component (normalized to albite), and 2 mol of H_2O per mole of alkali borate component (see London, 1986, Table 2). A model reaction for the crystallization of tourmaline from such a fluid may be expressed as

$$\begin{aligned} &\underset{\text{“hab”}}{3\ \mathrm{NaB_4O_5(OH)_4}} + \underset{\text{“py”}}{17\ \mathrm{Al_2Si_4O_9(OH)_4}} \\ &\quad = \underset{\text{“elbaite”}}{4\ \mathrm{Na(\square Al_8)(BO_3)_3Si_6O_{18}(OH)_4}} \\ &\qquad + \underset{\text{albite}}{2\ \mathrm{NaAlSi_3O_8}} + \underset{\text{quartz}}{38\ \mathrm{SiO_2}} + \underset{\text{V}}{32\ \mathrm{H_2O}}, \end{aligned}$$

in which "hab" and "py" represent hydrous alkali borate and pyrophyllite components of the melt. "Elbaite" (aluminous, iron-free tourmaline), albite, and quartz are crystallization products. In this model reaction, 8 mol of H_2O are liberated for every mole of tourmaline produced. The pocket shown in Figure 1A yielded approximately 21.2 kg of tourmaline (E. E. Foord, 1985, pers. comm.). By the above reaction, the crystallization of this quantity of tourmaline (at 460°C and 2500 bars) would have liberated approximately 4250 cm^3 of (pure) aqueous fluid (volumetric data for pure H_2O from Burnham et al., 1969). With a specific volume for elbaite = 0.33 cm^3/g, every 3 cm^3 of tourmaline crystallized by the above reaction at 460°C and 2500 bars creates approximately 2 cm^3 of fluid-filled void space.

To a large degree, the crystallization of tourmaline may govern the timing and extent of H_2O exsolution. Early and continuous crystallization of tourmaline buffers the activity of alkali borate to low values in hydrous silicate melts (Pichavant, 1981, 1983; Benard et al., 1985). Under these conditions, the crystallization of tourmaline should lead to steady devolatilization of silicate melt, with the result that an aqueous fluid may escape from the largely unconsolidated pegmatite. Observations presented here and elsewhere (e.g., London, 1984b, 1986), however, indicate that tourmaline commonly does not crystallize throughout much of the consolidation of pegmatitic systems, leading to high alkali borate contents in late-stage fluids. The causes of tourmaline instability are not fully known but may be functions of temperature, tourmaline crystal chemistry, the proportion of $^{IV}B/^{III}B$ coordination in pegmatitic fluids, and the general absence of ferromagnesian components in highly fractionated pegmatites (see the discussion in London, 1986). The accumulation of boron through fractional crystallization in the absence of tourmaline enhances the solubility (retention) of H_2O in late-stage fluids. The ultimate crystallization of abundant Al-rich tourmalines and consequent exsolution of H_2O from such late-stage fluids provides favorable conditions for pocket formation.

CONCLUSION

Miarolitic and massive rare-element pegmatites crystallize under similar *P-T* conditions. The magmatic-hydrothermal transition in miarolitic pegmatites occurs in the approximate ranges of 425–475°C and 2400–2800 bars. These conditions are consistent with the observed lithium aluminosilicate assemblages, fluid-inclusion data from the Kulam and San Diego pegmatites, and the peak metamorphic conditions attained by the host rocks of both pegmatite districts. Whether or not pockets form in pegmatites may be controlled largely by the activities of alkali borate melt components and, hence, by the timing of tourmaline crystallization. In miarolitic rare-element pegmatites such as those described in this paper, the crystallization of tourmaline does not occur until the late stages of pegmatite consolidation. Crystallization of tourmaline consumes an alkali borate fluxing component, which results in the deposition of other alkali aluminosilicate and oxide minerals, and the consequent exsolution of large amounts of H_2O. The deposition of tourmaline contributes directly to pocket formation by promoting the exsolution of an aqueous fluid phase. Vesiculation (pocket formation) is not restricted to the site of tourmaline crystallization but can occur anywhere in the pegmatitic fluid where the activity of alkali borate is diminished. Depending on the structural environment and the extent of pegmatite consolidation, the liberated aqueous fluid may form pockets or may be lost along fractures to react with crystallized pegmatite or host rocks. Field relations from miarolitic pegmatites (e.g., Foord et al., 1986) attest to a genetic link between pocket formation, late-stage boron-rich albitic liquids, and adjacent tourmalinization of wall rocks.

ACKNOWLEDGMENTS

George B. Morgan VI and Margaret A. Walsh assisted in the fluid-inclusion study of the Afghanistan pegmatites. Mike J. Holdaway performed the hydrothermal runs by which daughter-mineral reactions were monitored. The manuscript was carefully reviewed by Eugene E. Foord and an anonymous reviewer. Mineral samples from these pegmatites were provided by John S. White, Pete J. Dunn, and George E. Harlow.

This research was supported by a grant from the Oklahoma Mining and Mineral Resources Research Institute (Robert H. Arndt, director) of the U.S. Bureau of Mines (Allotment Grant G-1154140).

REFERENCES

Anderson, G.M., and Burnham, C.W. (1967) Reactions of quartz and corundum with aqueous chloride and hydroxide solutions at high temperatures and pressures. American Journal of Science, 265, 12–27.

Appleman, D.E., and Stewart, D.B. (1968) Crystal chemistry of spodumene-type pyroxenes. (abs.) Geological Society of America Special Paper 101, 5–6.

Benard, F., Moutou, P., and Pichavant, Michel. (1985) Phase relations of tourmaline leucogranites and the significance of tourmaline in silicic magmas. Journal of Geology, 93, 271–291.

Bodnar, R. J. (1983) A method of calculating fluid inclusion volumes based on vapor bubble diameters and the *P-V-T-X* properties of inclusion fluids. Economic Geology, 78, 535–542.

Bonniaud, R., Redon, A., and Sombret, C. (1978) Application of borate glasses and various boron bearing glasses to the management of French radioactive wastes. In L.D. Pye, V.D. Frenchette, and N.J. Kreidl, Eds. Borate glasses: Structure, properties, applications. Materials Science Research, 12, 597–616. Plenum Press, New York.

Burnham, C.W. (1967) Hydrothermal fluids at the magmatic stage. In H.L. Barnes, Ed. Geochemistry of hydrothermal ore deposits, first edition, 34–76. Holt, Rinehart, and Winston, New York.

Burnham, C.W., Holloway, J.R., and Davis, N.F. (1969) Thermodynamic properties of water to 1,000°C and 10,000 bars. Geological Society of America Special Paper 132.

Burnham, C.W., and Nekvasil, Hanna. (1986). Equilibrium properties of granite pegmatite magmas. American Mineralogist, 71, 239–263.

Cameron, E.N., and others. (1954) Pegmatite investigations, 1942–45, New England. U.S. Geological Survey Professional Paper 255.

Cassedanne, J.P., and Cassedanne, J.O. (1981) The Urubu pegmatite and vicinity. Mineralogical Record, 12, 73–77.

Chorlton, L.B., and Martin, R.F. (1978) The effect of boron on the granite solidus. Canadian Mineralogist, 16, 239–244.

Fisher, J.R. (1976) The volumetric properties of H_2O—A graphical portrayal. U.S. Geological Survey Journal of Research, 4 (2), 189–193.

Foord, E.E. (1976) Mineralogy and petrogenesis of layered pegmatite-aplite dikes in the Mesa Grande district, San Diego County, California. Ph.D. thesis, Stanford University, Stanford, California.

——— (1977) Famous mineral localities: The Himalaya dike system, Mesa Grande district, San Diego County, California. Mineralogical Record, 8, 461–474.

Foord, E.E., Starkey, H.C., and Taggart, J.E., Jr. (1986) Mineralogy and paragenesis of "pocket" clays and associated minerals in complex granitic pegmatites, San Diego, California. American Mineralogist, 71, 428–439.

Hollister, L.S., and Burruss, R.C. (1976) Phase equilibria in fluid inclusions from the Khtada Lake metamorphic complex. Geochimica et Cosmochimica Acta, 40, 163–175.

Jahns, R.H. (1979) Gem-bearing pegmatites in San Diego County. In P.L. Abbott and V.R. Todd, Eds. Mesozoic crystalline rocks: Peninsular Ranges batholith and pegmatites, Point Sal ophiolite, 3–38. Guidebook to field trips for the Geological Society of America Annual Meeting, published by the Department of Geological Sciences, San Diego State University, San Diego, California.

——— (1982) Internal evolution of pegmatite bodies. In Petr Černý, Ed. Granitic pegmatites in science and industry, 293–327. Mineralogical Association of Canada Short Course Handbook 8.

Jahns, R.H., and Burnham, C.W. (1969) Experimental studies of pegmatite genesis. I. A model for the derivation and crystallization of granitic pegmatites. Economic Geology, 64, 843–864.

Jahns, R.H., Tuttle, O.F. (1963) Layered pegmatite-aplite intrusives. Mineralogical Society of America Special Paper, no. 1, 78–92.

Jahns, R.H., and Wright, L.A. (1951) Gem- and lithium-bearing pegmatites of the Pala district, San Diego County, California. California Division of Mines Special Report, no. 7-A.

Jolliff, B.L., Papike, J.J., Shearer, C.K., and Laul, J.C. (1986) Tourmaline as a recorder of pegmatite evolution: Bob Ingersoll pegmatite, Black Hills, South Dakota. American Mineralogist, 71, 472–500.

London, David. (1983) The magmatic-hydrothermal transition in rare-metal pegmatites: Fluid inclusion evidence from the Tanco mine, Manitoba. (abs.) EOS (American Geophysical Union Transactions), 64, 549.

——— (1984a) Experimental phase equilibria in the system $LiAlSiO_4$-SiO_2-H_2O: A petrogenetic grid for lithium-rich pegmatites. American Mineralogist, 69, 995–1004.

——— (1984b) The role of lithium and boron in fluid evolution and ore deposition in rare-metal pegmatites. Geological Society of America Abstracts with Programs, 16, 578.

——— (1985) Origin and significance of inclusions in quartz: A cautonary example from the Tanco pegmatite, Manitoba: Economic Geology, 80, 1988–1995.

——— (1986) Magmatic-hydrothermal transition in the Tanco rare-element pegmatite: evidence from fluid inclusions and phase-equilibrium experiments. American Mineralogist, 71, 376–395.

London, David, and Burt, D.M. (1982) Lithium minerals in pegmatites. In Petr Černý, Ed. Granitic pegmatites in science and industry, 99–133. Mineralogical Association of Canada Short Course Handbook 8.

Norton, J.J. (1983) Sequence of mineral assemblages in differentiated granitic pegmatites. Economic Geology, 78, 854–874.

Pichavant, Michel. (1981) An experimental study of the effect of boron on a water-saturated haplogranite at 1 kbar vapour pressure. Contributions to Mineralogy and Petrology, 76, 430–439.

——— (1983) Melt-fluid interaction deduced from studies of silicate-B_2O_3-H_2O systems at 1 kbar. Bulletin de Minéralogie, 106, 201–211.

Potter, R.W., II, Clynne, M.A., and Brown, D.L. (1978) Freezing point depression of aqueous sodium chloride solutions. Economic Geology, 73, 284–285.

Roedder, Edwin. (1981) Natural occurrence and significance of fluids indicating high pressure and temperature. Physics and Chemistry of the Earth, 13, 9–39.

Roedder, Edwin, and Bodnar, R.J. (1980) Geologic pressure determinations from fluid inclusion studies. Annual Reviews of Earth and Planetary Sciences, 8, 263–301.

Rossovskii, L.N. (1977) First finding of pollucite and its crystals in Afghanistan (in Russian). Akademii Nauk SSSR Doklady, 236 (1), 216–219 (transl. Reports of the Academy of Science, USSR, Earth Science Sections, 236 (1), 157–160, 1977).

——— (1981) Rare-element pegmatites with precious stones and conditions of their formation (Hindu Kush) (in Russian). Zapiski Vsesoyuznogo Mineralogicheskogo Obshchestva, 109, 301–311 (transl. International Geology Review, 23, 1312–1320, 1981).

Rossovskii, L.N., Chmyrev, W.M., and Salakh, A.S. (1975) New finds and belts of rare-metal pegmatites in the Hindu Kush (Eastern Afghanistan) (in Russian). Geologiya Rudnykh Mestorozhdeniy, 17 (5) 102–106 (transl. International Geology Review, 18, 1339–1342, 1976).

Rossovskii, L.N., Makagon, V.M., and Kuz'mina, T.M. (1978) Characteristics of the formation of a kunzite deposit in Afghanistan (in Russian). Geologiya i Geofizika, 19 (11), 102–109 (transl. Soviet Geology and Geophysics, 19 (11), 82–87, 1978).

Rossovskii, L.N., and Shmakin, B.M. (1978) Unique example of vertical geochemical zoning in pegmatites of the Hindu Kush, Afghanistan (in Russian). Akademii Nauk SSSR Doklady, 240 (2), 448–451 (transl. Reports of the Academy of Science, USSR, Earth Science Sections, 240, 204–206, 1978).

Taylor, B.E., Foord, E.E., and Friedrichsen, H. (1979) Stable isotope and fluid inclusion studies of gem-bearing granitic pegmatite-aplite dikes, San Diego County, California. Contributions to Mineralogy and Petrology, 68, 187–205.

Todd, V.R., and Shaw, S.E. (1979) Structural, metamorphic, and intrusive framework of the Peninsular Ranges batholith in southern San Diego County, California. In P.L. Abbott and V.R. Todd, Eds. Mesozoic crystalline rocks: Peninsular Ranges batholith and pegmatites, Point Sal ophiolite, 177–231. Guidebook to field trips for the Geological Society of America Annual Meeting, published by the Department of Geological Sciences, San Diego State University, San Diego, California.

Touret, Jaques (1981) Fluid inclusions in high-grade metamorphic rocks. In L.S. Hollister and M.L. Crawford, Eds. Fluid inclusions: Applications to petrology, 182–208. Mineralogical Association of Canada Short Course Handbook 6.

Walker, R.J. (1985) The origin of the Tin Mountain pegmatite, Black Hills, South Dakota. Ph.D. thesis, South Dakota School of Mines, Rapid City.

MANUSCRIPT RECEIVED JULY 19, 1985
MANUSCRIPT ACCEPTED OCTOBER 21, 1985